Engineering Research Express

PAPER • **OPEN ACCESS**

Impact monitoring of CFRP composites with acoustic emission and laser Doppler vibrometry

To cite this article: S Grigg *et al* 2021 *Eng. Res. Express* **3** 015012

IOP Publishing Eng. Res. Express 3 (2021) 015012 https://doi.org/10.1088/2631-8695/abde8b

Engineering Research Express

CrossMark

OPEN ACCESS

RECEIVED
15 October 2020

REVISED
5 January 2021

ACCEPTED FOR PUBLICATION
21 January 2021

PUBLISHED
4 February 2021

PAPER

Impact monitoring of CFRP composites with acoustic emission and laser Doppler vibrometry

S Grigg , F Almudaihesh , M Roberts and R Pullin
Cardiff School of Engineering, Cardiff University, Cardiff, United Kingdom
E-mail: griggs@cardiff.ac.uk

Keywords: acoustic emission, laser Doppler vibrometry, composites, impact

Abstract

The use of Acoustic Emission (AE) to detect impacts is of interest within industries where vital components are prone to impact damage, in particular where Carbon Fibre Reinforced Polymers (CFRP) are used, as damage can often go un-noticed within them. For AE monitoring of impacts piezoelectric sensors are used to detect the ultrasonic wave produced by an impact. Classification is also possible of these waves enabling a distinction between damaging and non-damaging impacts. These sensors do however have resonance, so do not give an accurate picture of how the waves propagate, better knowledge would enable better selection of sensors. Laser Doppler Vibrometry is a non-contact and non-resonant method of analysing the surface displacement on a structure. In this study, a vibrometer was used to monitor CFRP plates during impact to assess its applicability for distinguishing between damaging and non-damaging impacts, compared with a surface mounted AE sensor. The vibrometer was able to detect both low frequency flexural modes due to the impact process and the higher frequency extensional modes, initiated by damage. When compared to the AE sensor the vibrometer was comparable in its results, and unlike the sensor, not susceptible to resonance or decoupling. For the tested material the vibrometer identified frequencies greater than 20 kHz to be associated with damaging impacts.

1. Introduction

The use of Carbon Fibre Reinforced Polymer (CFRP) composites is increasing significantly in the aerospace, automotive, and marine industries due to their high strength-to-weight and stiffness-to-weight ratios compared with metallic structures. They also benefit from excellent fatigue and corrosion resistance properties [1]. However their inherent reaction to external dynamic excitations, such as structural impacts, is still a significant concern in real life application where threatening internal damage, such as delamination and interfacial debonding, can exist and not be visually detectable [2, 3].

Traditional Non-Destructive Testing (NDT) techniques, such as ultrasonic imaging, thermography and holograph, are effective for detecting damage in composites; however, typically do require the structure to be out of service, causing inconvenience and cost [4–6]. It is therefore essential to develop NDT techniques to help monitor structures during real life operations [7]. Structural Health Monitoring (SHM) is promising due to its ability to possess self-sensing capability to continually monitor structures during service [8, 9].

One SHM approach that has been investigated for detecting impact damage in composites is the *in situ* monitoring of Acoustic Emission (AE). AE is the spontaneous release of energy due to the growth of damage that propagates as a high frequency (kHz—MHz) elastic wave through a structure, the monitoring of which enables the detection of damage [10]. Researchers have also shown it is possible to locate the location of an impact through triangulation techniques [11, 12]. How this wave propagates and at what frequency is dependent on a number of factors, including the material type and shape of the structure. For this study, thin plates are being used; hence, waves will propagate as Lamb waves, which exist through the plate's thickness [13]. There are two main types of mode in which a Lamb wave forms; these are referred to as flexural or extension modes, the difference being the wave forming symmetrically or antisymmetrically through the structure [14]. These waves are dispersive, meaning their velocity is dependent on frequency, with extensional modes typically travelling faster and at a higher frequency.

Authors have identified a strong relationship between impact energy and the AE produced. A low energy, non-damaging, impact on a composite primarily produces a low frequency, slower, flexural wave mode. When damage is initiated a higher frequency extensional mode is generated, which has been shown to increase relative to the stress wave with increased damage size [15, 16]. Better understanding of the waves and frequencies associated with damage allows better characterisation as to whether a signal is a result of a damaging or non-damaging impact.

In previous studies AE has been collected using a range of piezo-electric sensors, including wideband [15–17] and resonant [18]. Use of a physical sensor is required in order to monitor AE for any in service application. However, there are disadvantages in doing this, primarily that the resonance of the sensor itself alters the frequencies of the recorded wave, with even wideband sensors having some resonance. This makes any spectral analysis conducted and therefore conclusions drawn from them, flawed. The act of attaching any sensor also has the potential to add damping to the structure, altering the wave propagation.

Laser Doppler Vibrometry (LDV) is a method of measuring the velocity of surface displacement on a structure. It does this by analysing the change in frequency and phase within the backscattered laser reflected from a surface; this change is the result of structural vibration causing Doppler shift within the laser [19]. Researchers have used LDV for a range of NDT applications, including modal analysis [20, 21] and acousto-ultrasonic inspection [22–24], however to the best knowledge of the authors, not for assessing high frequency AE from impact damage in composites.

This paper presents the results from low velocity impact testing on CFRP monitored with both a physical AE sensor and LDV. Further frequency analysis has been performed on the data, extracting and quantifying the flexural and extension modes present within the signals. This data has been analysed and trends identified, which correspond with those from literature. The ability of the LDV to distinguishing between damaging and non-damaging impacts could assist to define the frequency characteristics of an ideal transducer for monitoring impacts.

2. Experimental methods

2.1. Materials

Unidirectional prepreg with 300 g m^{-2} HT carbon fibre/38% RP507 resin was used in this study. The materials were cured as recommended by the material supplier, using an autoclave for two hours at 120 °C and five bar pressure. Three panels with dimensions of 280 mm by 280 mm, consisting of 16 plies (3.53 mm total thickness) with a layup of $[0/90]_{8s}$ were prepared to apply differing impact damage energies. The dimensions were selected to ensure separation of initial wave-front and edge reflections, when recorded by the vibrometer and AE sensor. The stacking sequence was implemented to simplify the damage mechanism by excluding additional fibre directions.

2.2. Acoustic emission

A resonant Pancom Pico-Z sensor was used to collect AE, which has been shown to be effective for detecting and locating impacts in composites [25]. As can be seen in figure 1, the frequency response of this sensor is poor below 100 kHz, and relatively flat from 200–500 kHz. Data was recorded on a reference channel within the vibrometer at a sample rate of 2.56 MHz. The sensor was bonded 70 mm from the impact location on the underside of the specimen, at 0° from the impact. This distance was chosen as it made the sensor equidistant from the impact location and the edge of the panel, as shown in figure 2.

2.3. Laser vibrometer

In this study a single laser head from a Polytec PSV-500-3D was used to perform an out of plane single point measurement. The light was directed to a point 70 mm from the impact point on the underside of the specimen at 180° from the impact location, the opposite side to the AE sensor, as shown in figure 2. The laser was directed to the panel using a front surface mirror at an angle of 45° which, unlike a conventional mirror, does not refract the light. This setup is shown in figure 3. A 10 mm square of retroreflective tape was bonded at the measurement point to ensure the adequate backscatter of light. Like the reference channel the vibrometer was sampling at 2.56 MHz.

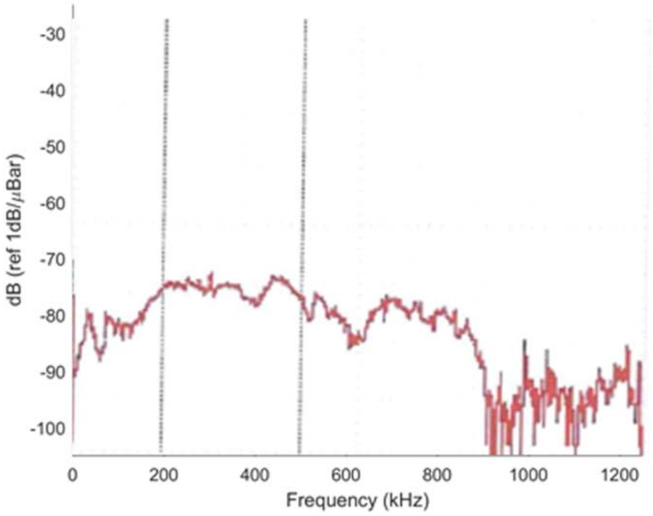

Figure 1. Frequency response of Pico-Z sensor. Figure modified for clarity from the manufactures supplied calibration certificate, where the trace was acquired using face-to-face excitation with a Panametrics-NDT sensor type V103 pulsed with 20 volts pp & 50 nS rise time. Adapted with the permission of PANCOM Ltd.

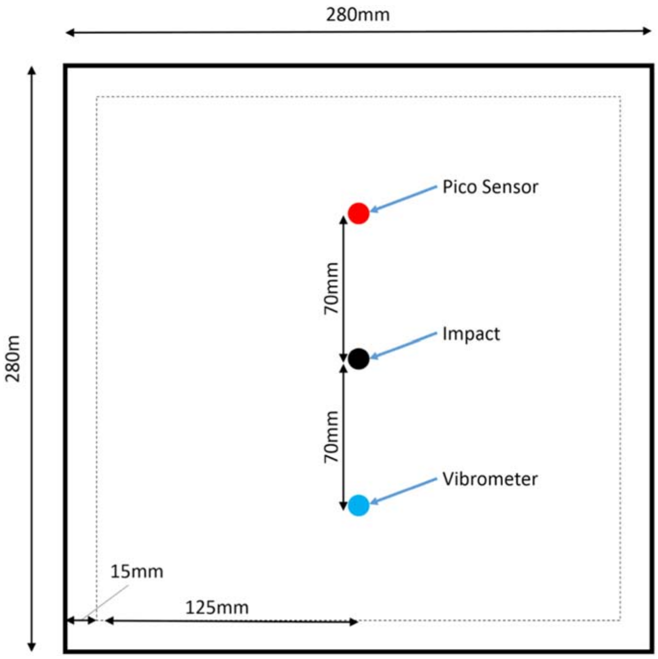

Figure 2. Layout of composite specimen in impact rig. Dashed lines indicate restrained area.

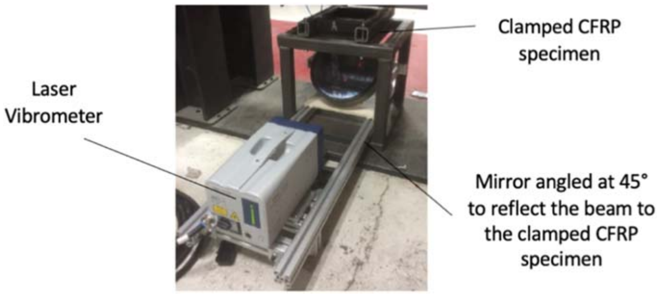

Figure 3. Impact test configuration.

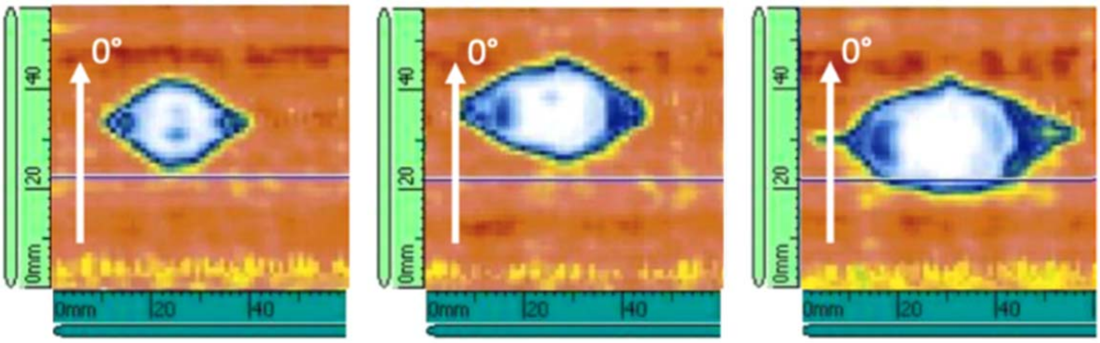

(A) (B) (C)

Figure 4. Observed ultrasonic phased array C-Scans; (A) 30 J, (B) 40 J, and (C) 50 J.

Table 1. The maximum load and damage size observed after 30 J, 40 J and 50 J impact.

Impact energy (J)	Maximum load (N)	Damage size (mm^2)
30	1254	410
40	1546	600
50	1673	800

2.4. Ultrasonic testing

The ability of ultrasonic waves to propagate in composite materials enables detection of damage location and size [26]. Phased Array scanning is a handheld ultrasonic NDT technique, that can detect the presence of damage in composite structures, such as delamination and debonding [27, 28]. This is achieved through the pulsing of ultrasonic waves from transducers in a linear array. The response of the back surface is then taken. The presence of damage within the structure will result in a drop in amplitude of the returned signal. The stacking of these readings over a period of time, or by position using an encoder, allows a top down view of the plate to be produced, which is known as a C-Scan.

For internal damage assessment in this study, an OmniScan MX2 ultrasonic Phased Array system supplied by OLYMPUS was used. A 5L64-NW1 probe was used, which consists of 64 5 MW transducers, this was combined with a SNW1-0L-AQ25 wedge and wheel encoder, allowing to scale sizing of damage in 2D. The software ImageJ2 [29] was then used on the produced C-scans to find an approximation of the damage size.

2.5. Impact damage

To investigate the AE produced by low velocity impacts, three of the CFRP panels made were impacted with energies of 30 J, 40 J, and 50 J. The specimens were clamped in a customized rig to hold the CFRP specimen; 15 mm of the four side edges were clamped leaving 250 mm by 250 mm of the specimen exposed to impact, as shown in figure 2. The laser vibrometer and a front surface mirror angled at 45° to reflect the laser vibrometer beam to CFRP specimen were also mounted on the fixture as shown in figure 3. The distance between the front of the laser head and the mirror was 850 mm, and the distance between the reflected beam and the CFRP specimen was 500 mm. The impact was applied using an Instron 9250-HV drop tower, with a 16 mm (± 0.1) diameter hemispherical impactor and a mass of 5.5 kg. A built-in load cell enabled recording of the load response through the impactor. A trial specimen identical to the others was prepared and impacted with 3 J energy to verify the test set-up.

3. Results and discussions

Barely visible impact damage on the external surface was observed in all specimens impacted with higher energy. The internal damage is however clearly seen in all specimens where the extent of internal damage increases with the increase in impact energy as presented in figure 4. Table 1 shows the approximate damage area for each test, predicted using ImageJ2, and the maximum load observed by the load cell within the impact test rig.

Figure 5 shows the normalised voltages of the Pico-Z sensor and the vibrometer in relation to the observed load under 30 J, 40 J and 50 J impact for all specimens. The data has been normalised to allow for better

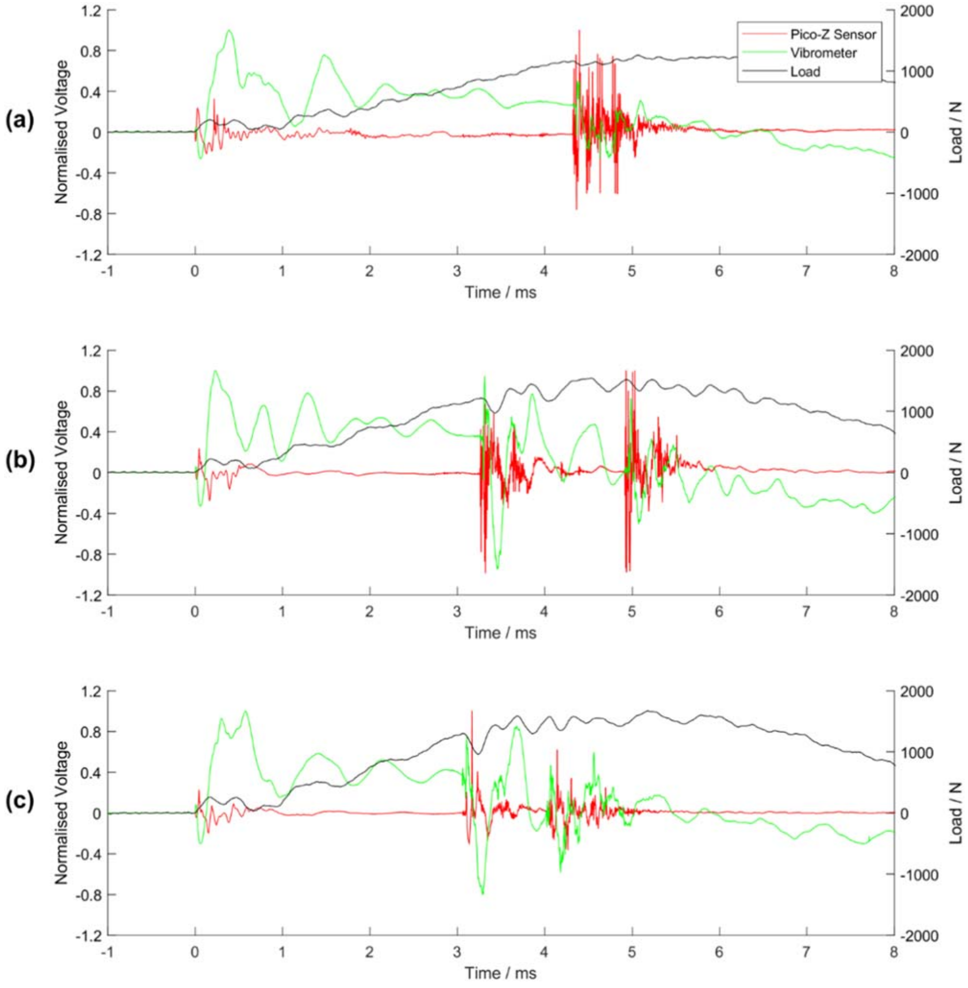

Figure 5. Normalised voltage for vibrometer (green) and Pico-Z sensor (red) plotted alongside load data (black) for 30 J (a), 40 J (b) and 50 J (c) impact energy.

presentation. This is because the voltage outputs for each device are very different, making non-normalised values difficult to visualise, and any frequency analysis incomparable. The vibrometer can be seen to have detected substantially more low frequency flexural mode compared with the Pico-Z sensor. This is to be expected due to the sensor's poor response at low frequencies, as shown in figure 1.

High frequency waves in figure 5 can be seen to correspond with drops in load, which is known to be a result of damage. The Pico-Z sensor received significantly higher levels of high frequency waves. This is shown clearly in figure 6, where a 1 ms period of the two normalised waves are shown side by side, with vibrometer only detecting minimal higher frequency. This is attributed to the resonance of the Pico-z sensor. The FFT in figure 7 confirms minimal high frequency content within the vibrometer data. The high frequency component recorded by the Pico-Z sensor is outside its highest response region of 200 kHz–500 kHz, as shown in figure 1; however, does match well with a sub peak in response around 100 kHz.

Presented in figure 8(a) is a comparison of a vibrometer recording from an impact that caused substantial damage (30 J) with a trial specimen which was impacted with only 3 J where no damage was seen from phased array data. The 30 J impact had a peak amplitude four times higher than that of the 3 J impact. However, after normalisation, the initial 1 ms of wave, where only flexural mode is present, was very similar, indicating that prior to the initiation of damage the waves produced are similar when scaled. This is supported by the FFT results in figure 8(b) which show that below 10 kHz the signals are very similar. However, above this, there is a clear difference in the frequency content of the two waveforms, with the 3 J impact having little signal above 20 kHz. This supports the findings of Mahdian *et al* [16] where waves of this frequency were associated with the impact process, but not damage.

As the vibrometer detected significantly greater low frequency flexural mode than the AE sensor, it was difficult to compare the extensional modes. In order to do this the waveforms were passed through an Infinite Impulse Response (IIR) high pass digital filter with a pass frequency of 20 kHz and a Butterworth window. Figure 9 shows the normalised output of the filters on the vibrometer and Pico-Z sensor waveforms for each of

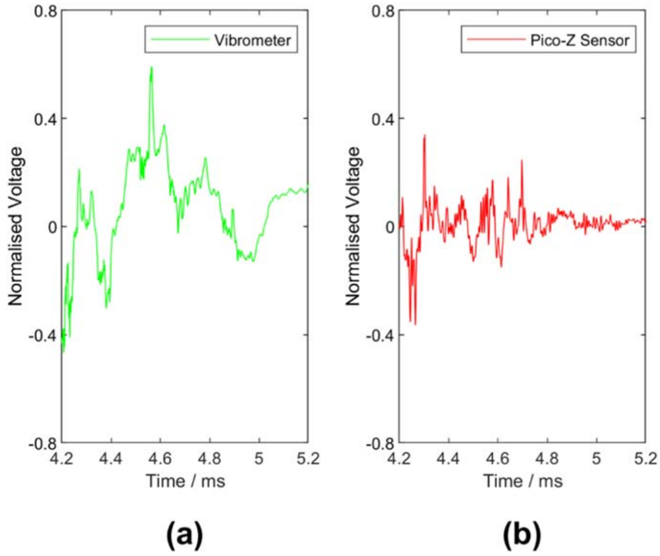

Figure 6. One millisecond extract of normalised voltage for vibrometer (a) and Pico-Z sensor (b) for 30 J impact.

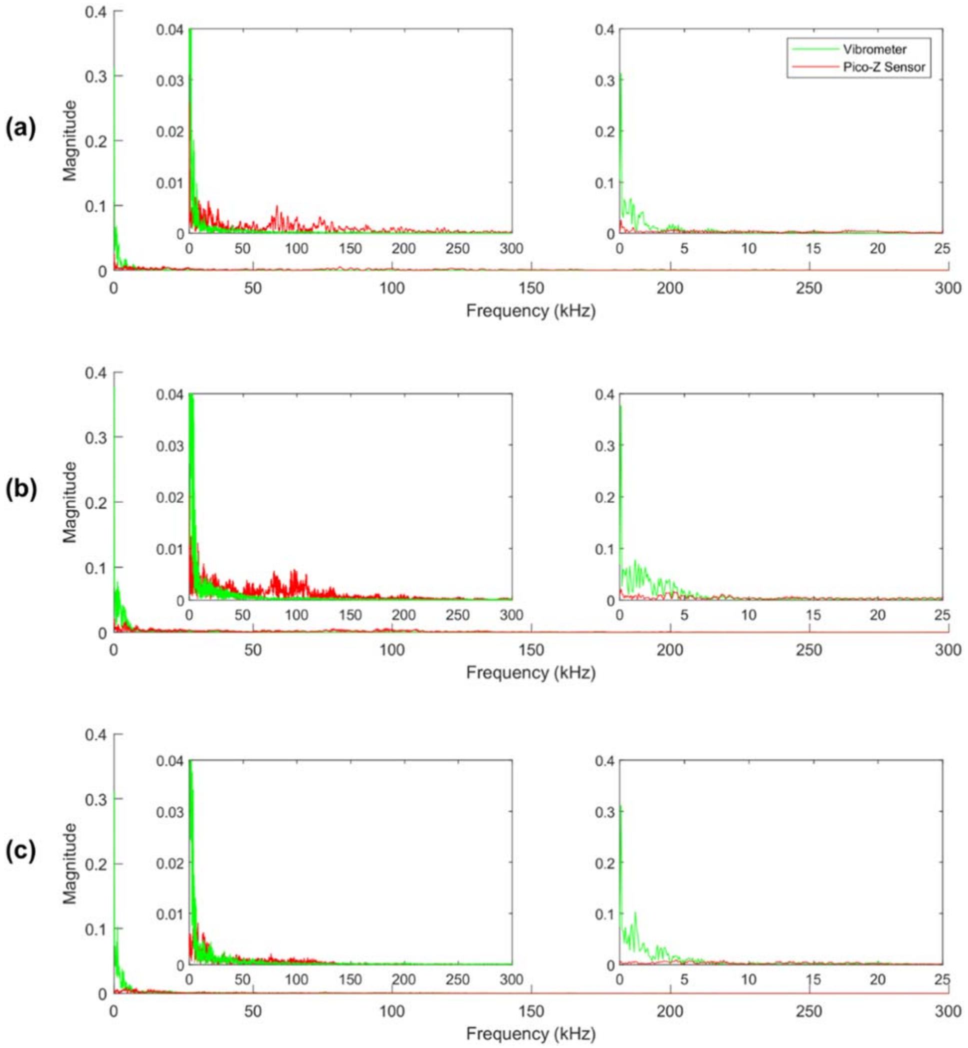

Figure 7. FFT results of normalised waveforms from laser vibrometer reading (green) and Pico-Z sensor for 30 J (a), 40 J (b) and 50 J (c) impacts. Zoomed in plots with reduced X and *Y* axis also included in each.

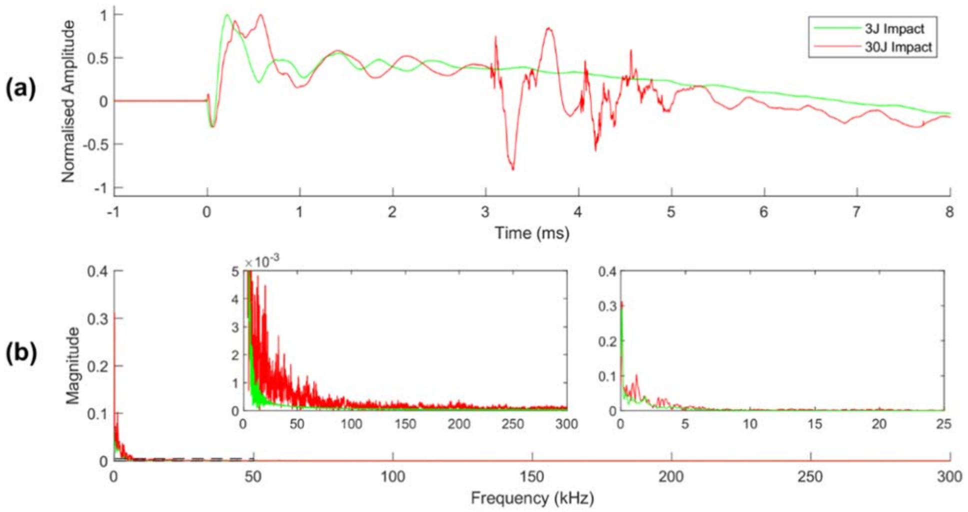

Figure 8. Normalised vibrometer waveforms for 3 J impact (green) and 30 J impact (red) (a) and an FFT of the two impacts (b).

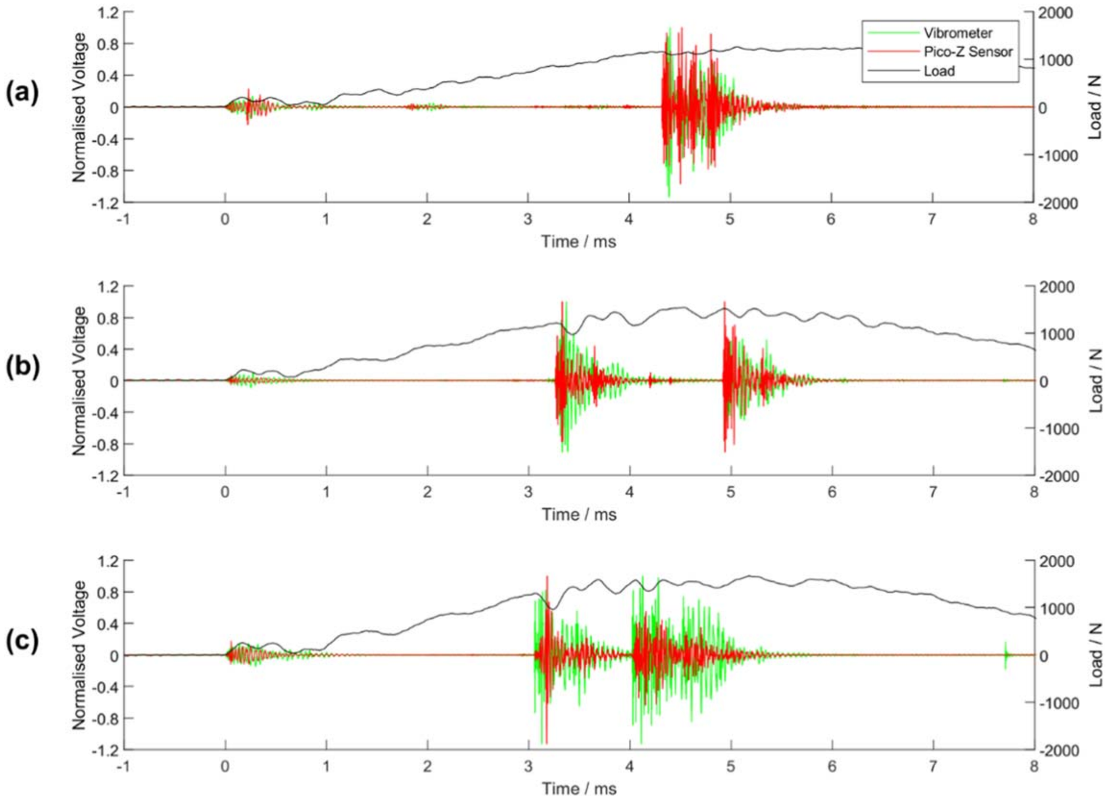

Figure 9. Normalised voltage for vibrometer (green) and Pico-Z sensor (red) after a 20 kHz high pass filter, plotted alongside load data (black) for 30 J (a), 40 J (b) and 50 J (c) impact energy.

the 30 J, 40 J and 50 J impacts. Although significantly different in amplitudes, when normalised, as they have been in figure 9, the two observed signals showed very similar trends; however, are not identical signals. This difference is likely to be a result of the resonance of the sensor, its damping on the panel and any inconsistencies in the panels caused by the two different locations.

Table 1 shows that an increase in impact energy caused both an increase in force through the impactor, and an increased damage size. The absolute Root Mean Square (RMS) of the raw signals acquired from the Pico-Z sensor and vibrometer, compared to impact energy, are shown in figure 10(a). The absolute energy of the signals after the 20 kHz high pass filter is shown in figure 10(b). The 3 J trial impact has also been included in these plots.

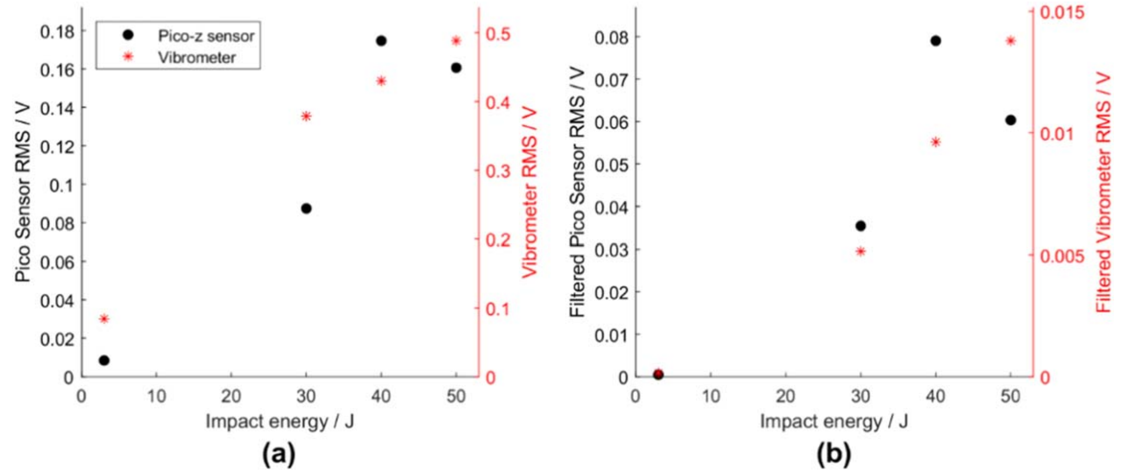

Figure 10. RMS of Pico-Z and vibrometer waveforms compared to impact energy (a) and filtered waveforms (b).

Although as the number of data points is severely limited, so making any conclusions difficult to draw with certainty, the data in figure 10 shows that the Pico-Z AE sensor data has a likely outlier, either the 40 J or 50 J impact. It is believed that the 50 J is the outlier as in figure 9(c) the energy of the Pico-Z compared to the vibrometer is much lower, whereas in (a) and (b), it matches much better. This is further supported by the lower high frequency content in the signal, shown in figure 7(c). Calibration testing confirmed that the sensor was bonded correctly and not damaged prior to the test, meaning the most likely problem was that the high impact energy caused the sensor to partially decouple, and so have a lower response. For these reasons only, the vibrometer data will be considered in the following discussion.

From the work of Mahdian *et al* [16], it is known that AE waveforms will have low frequency content due to the impact process. Figure 10(a) demonstrates that this was the case at low energy and increased as the impact energy was greater. The limited number of data points makes trends difficult to identify reliably; however, the three higher impact energies can be seen to have a relatively linear relationship. More data points would be required in order to adequately predict the trend of AE RMS versus impact energy. This trend would not be expected to be linear throughout, due to delamination and fibre breakage taking place and absorbing energy, so reducing the rate that wave RMS increases as impact energy is increased [30, 31].

For the filtered data in figure 10(b), like the unfiltered data if only considering the high impact data points, a linear relationship exists. The 3 J impact does not fit the trend, and is near zero, due to its minimal high frequency content, as shown in figure 8. Further testing at impact energies between 3 J and 30 J would identify the relationship, and at what impact energy high frequency waves began to be observed by the vibrometer.

The selection of the Pico-Z sensor for this testing was based on previous literature and not commercially designed for the purpose of detecting damaging impact. This sensor did successfully distinguish between damaging and non-damaging impacts; however, careful selection would enable more sensitivity to smaller damage as well as increasing the range and probability of detection. Specifying a sensor’s ideal frequency response is very dependent on the structure: the material and its thickness having a major influence on the frequency of wave propagation. Within this testing of a non-damaging impact, the laser vibrometer identified no significant waves with a frequency greater than 20 kHz. Although more substantial testing is required with further testing conducted between 3 J and 30 J, this result indicates that one option for a damage detection system would be to filter this low frequency. This could be done through tailored sensor response, front end filters or digital filters, which could enable better identification on damaging impacts. It should also be considered that any change to the structure may affect these results. Therefore, further testing of different thicknesses should be investigated using a laser vibrometer to quantify it.

The application of the approached used in this testing applied to real composite structures, such as those in aerospace and on wind turbines, would enable the better detection of impact damage by increasing the range of sensors and reducing false positives.

4. Conclusions

This work presents the first reported use of a LDV to monitor the response of composite panels during low velocity impacts, both damaging and non-damaging. The vibrometer was shown to not only be effective at doing this, but more reliable than an AE sensor, which was influenced by its resonance, and at risk of decoupling during impact. This makes the laser vibrometer a promising tool. Further testing would better reinforce the trends presented within this paper, which are as expected. The use of a laser vibrometer for monitoring of impacts in test situations gives a better understanding of the high frequency waves produced as a result of damage, enabling better selection of AE sensors for real application and identification of damaging impacts.

Data availability statement

The data that support the findings of this study are available upon reasonable request from the authors.

Funding

This work was funded through the Airbus Endeavr Wave collaboration between Airbus, Cardiff University and the Welsh Government.

ORCID iDs

S Grigg https://orcid.org/0000-0002-5317-7139
F Almudaihesh https://orcid.org/0000-0001-9360-9672

References

[1] Agarwal B, Broutman L and Chandrashekhara K 2006 *Analysis and Performance of Fiber Composites* (New York: Wiley)
[2] Richardson M O W and Wisheart M J 1996 Review of low-velocity impact properties of composite materials *Compos. Part A Appl. Sci. Manuf.* **27** 1123–31
[3] Agrawal S, Singh K K and Sarkar P K 2014 Impact damage on fibre-reinforced polymer matrix composite—a review *J. Compos. Mater.* **48** 317–32
[4] Ren W, Liu J, Tian G Y, Gao B, Cheng L and Yang H 2013 Quantitative non-destructive evaluation method for impact damage using eddy current pulsed thermography *Compos. Part B Eng.* **54** 169–79
[5] Ramadas C, Padiyar J, Balasubramaniam K, Joshi M and Krishnamurthy C V 2011 Lamb wave based ultrasonic imaging of interface delamination in a composite T-joint *NDT E Int.* **44** 523–30
[6] Pagliarulo V *et al* 2015 Impact damage investigation on composite laminates: comparison among different NDT methods and numerical simulation *Meas. Sci. Technol.* **26** 085603
[7] Measures R M 1992 Smart composite structures with embedded sensors *Compos. Eng.* **2** 597–618
[8] Leng J and Asundi A 2003 Structural health monitoring of smart composite materials by using EFPI and FBG sensors *Sensors Actuators A Phys.* **103** 330–40
[9] Fu T, Liu Y, Lau K T and Leng J 2014 Impact source identification in a carbon fiber reinforced polymer plate by using embedded fiber optic acoustic emission sensors *Compos. Part B Eng.* **66** 420–9
[10] Liu M, Wang Q, Zhang Q, Long R and Su Z 2018 Characterizing hypervelocity (>2.5 km/s)-impact-engendered damage in shielding structures using *in situ* acoustic emission: simulation and experiment *Int. J. Impact. Eng.* **111** 273–84
[11] Kundu T, Das S and Jata K V 2009 Detection of the point of impact on a stiffened plate by the acoustic emission technique *Smart Mater. Struct.* **18** 035006
[12] Perelli A, De Marchi L, Marzani A and Speciale N 2012 Acoustic emission localization in plates with dispersion and reverberations using sparse PZT sensors in passive mode *Smart Mater. Struct.* **21** 025010
[13] Lamb H 1917 On waves in an elastic plate *Proc R Soc London Ser A* **93** 114–28
[14] Ciampa F and Meo M 2010 Acoustic emission source localization and velocity determination of the fundamental mode A0 using wavelet analysis and a Newton-based optimization technique *Smart Mater. Struct.* **19** 045027
[15] Prosser W, Gorman M and Humes D 1999 Acoustic emission signals in thin plates produced by impact damage *J. Acoust. Emiss.* **17** 29–36
[16] Mahdian A, Yousefi J, Nazmdar M, Zarif Karimi N, Ahmadi M and Minak G 2017 Damage evaluation of laminated composites under low-velocity impact tests using acoustic emission method *J. Compos. Mater.* **51** 479–90
[17] Saeedifar M, Najafabadi M A, Zarouchas D, Toudeshky H H and Jalalvand M 2018 Barely visible impact damage assessment in laminated composites using acoustic emission *Compos Part B Eng* **152** 180–92
[18] Sung D U, Kim C G and Hong C S 2002 Monitoring of impact damages in composite laminates using wavelet transform *Compos Part B Engineering* **33** 35–43
[19] Chen D-M and Zhu W D 2017 Investigation of three-dimensional vibration measurement by a single scanning laser Doppler vibrometer *J. Sound Vib.* **387** 36–52
[20] Stanbridge A B and Ewins D J 1999 Modal testing using a scanning laser Doppler vibrometer *Mech. Syst. Signal Process* **13** 255–70
[21] Rothberg S J *et al* 2017 An international review of laser Doppler vibrometry: making light work of vibration measurement *Opt. Lasers Eng.* **99** 11–22
[22] Staszewski W J, Mahzan S and Traynor R 2009 Health monitoring of aerospace composite structures—active and passive approach *Compos. Sci. Technol.* **69** 1678–85
[23] Marks R, Gillam C, Clarke A, Armstrong J and Pullin R 2017 Damage detection in a composite wind turbine blade using 3D scanning laser vibrometry *Proc. Inst. Mech. Eng. Part C J. Mech. Eng. Sci.* **231** 3024–41
[24] Staszewski W J, Lee B C and Traynor R 2007 Fatigue crack detection in metallic structures with Lamb waves and 3D laser vibrometry *Meas. Sci. Technol.* **18** 727

[25] Eaton M, Pearson M, Holford K, Featherston C and Pullin R 2012 Detection and location of impact damage using acoustic emission *Proc. Second Int. Conf. Adv. Compos. Mater. Technol. Aerosp. Appl.* pp 29–33

[26] Towsyfyan H, Biguri A, Boardman R and Blumensath T 2020 Successes and challenges in non-destructive testing of aircraft composite structures *Chinese J Aeronaut.* **33** 771–91

[27] Freemantle R J, Hankinson N and Brotherhood C J 2005 Rapid phased array ultrasonic imaging of large area composite aerospace structures *Insight Non-Destructive Test Cond. Monit.* **47** 129–32

[28] Yuan C, Xie C, Li L, Zhang F and Gubanski S M 2016 Ultrasonic phased array detection of internal defects in composite insulators *IEEE Trans. Dielectr. Electr. Insul.* **23** 525–31

[29] Rueden C T *et al* 2017 ImageJ2: imageJ for the next generation of scientific image data *BMC Bioinf.* **18** 1–26

[30] Gómez-del Río T, Zaera R, Barbero E and Navarro C 2005 Damage in CFRPs due to low velocity impact at low temperature *Compos. Part B Eng.* **36** 41–50

[31] Delfosse D and Poursartip A 1997 Energy-based approach to impact damage in CFRP laminates *Compos. Part A Appl. Sci. Manuf.* **28** 647–55